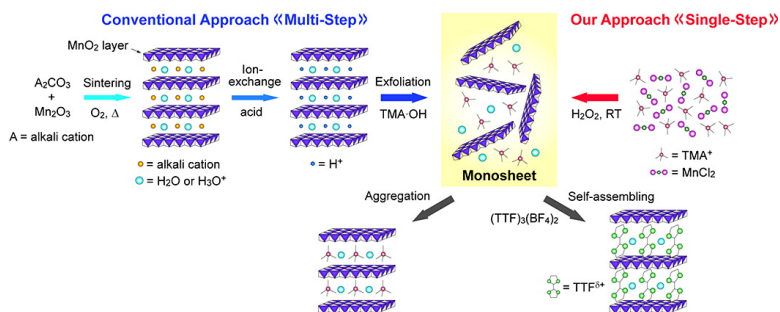## Article

Room-Temperature Synthesis of Manganese Oxide Monosheets

Kazuya Kai, Yukihiro Yoshida, Hiroshi Kageyama, Gunzi
Saito, Tetsuo Ishigaki, Yu Furukawa, and Jun Kawamata

More About This Article

Additional resources and features associated with this article are available within the HTML version:

- Supporting Information
- Access to high resolution figures
- Links to articles and content related to this article
- Copyright permission to reproduce figures and/or text from this article

View the Full Text HTML

Room-Temperature Synthesis of Manganese Oxide Monosheets

Kazuya Kai,[†] Yukihiro Yoshida,*,[†] Hiroshi Kageyama,[†] Gunzi Saito,*,[†,‡]
Tetsuo Ishigaki,[§] Yu Furukawa,[§] and Jun Kawamata[§]

*Division of Chemistry, Graduate School of Science, Kyoto University, Sakyo-ku,
Kyoto 606-8502, Japan, Research Institute, Meijo University, Shiogamaguchi 1-501 Tempaku,
Nagoya 468-8502, Japan, and Department of Chemistry, Faculty of Science, Yamaguchi
University, Yoshida 1677-1, Yamaguchi 753-8512, Japan*

Received June 13, 2008; E-mail: yoshiday@kuchem.kyoto-u.ac.jp; saito@kuchem.kyoto-u.ac.jp

Abstract: Preparation of single-layer manganese oxide nanosheets (monosheets) comprised of edge-shared MnO_6 octahedra has relied on multistep processing involving a high-temperature solid-state synthesis of bulk templates, and ion-exchange and exfoliation reactions in solutions, requiring high cost and long processing time. Here we demonstrate the first single-step approach to directly access the MnO_2 monosheets, by the chemical oxidation of Mn^{2+} ions in the presence of tetramethylammonium cations in an aqueous solution. Of importance is that this template-free reaction readily proceeds within a day at room temperature. The ability of the MnO_2 monosheets to self-assemble allows aggregation, to form layered structures with potassium cations and cationic tetrathiafulvalene analogues as intercalants. Furthermore, Langmuir−Blodgett (LB) films composed of the MnO_2 monosheets were successfully fabricated by the LB deposition method, in which about one layer of the monosheets was deposited for each process.

1. Introduction

Nanosized materials with different morphologies, such as nanoparticles and clusters (zero-dimension, e.g., fullerenes), and nanotubes and nanowires (one-dimension, e.g., carbon nanotubes), have become increasingly important as potential systems for both fundamental interests and industrial applications.[1,2] Nanosheets are a new class of two-dimensional nanomaterials that are characterized by a thickness on the order of nanometers and lateral dimensions of submicro- to micrometers.[3,4] So far, a wide variety of transition-metal oxide nanosheets such as $Ca_2Nb_3O_{10}$,[5] Nb_6O_{17},[6] $Ti_{1-\delta}O_2$,[7] and MnO_2,[8] to name only a few, have been discovered and investigated extensively due to the rich chemistry and physics of the bulk counterparts.[3,4] The utmost feature of the nanosheets is their exceptionally high specific surface area, rendering them promising candidates for a variety of applications, especially in photocatalysis and electrodes of electrochemical devices.[3,4] Furthermore, the ability

of the nanosheets to self-assemble allows formation of restacked lamellar aggregates with a disordered and porous nature,[9] leading to enhanced properties as found in $H_4Nb_6O_{17}$[10] and $HTiNbO_5$[11] for photocatalysis, Li/MnO_2[12] for electrodes of lithium-ion batteries, and $H/RuO_{2.1}$[13] for double-layer capacitors.

However, several hurdles must be overcome before possible future applications can be realized. The synthesis of metal oxide nanosheets, until very recently, has required multistep processing, involving a high-temperature solid-state reaction (to yield a thermodynamically stable precursor phase, e.g., K/MnO_2), protonation of interlayer alkali metal ions (to yield, e.g., H/MnO_2), and an acid−base reaction with an aqueous solution of quaternary ammonium cations (to finally yield negatively charged nanosheets, e.g., $MnO_2^{\delta-}$ in the form of a colloidal suspension). This top-down approach is costly and time-consuming. Moreover, it is fairly difficult to exfoliate the protonated compounds completely into single-layer nanosheets (monosheets). In practice, previously obtained nanosheets possess a wide thickness distribution. It is highly desirable to obtain monosheets as a main product, because they possess a large specific surface area and also serve as primitive building units to construct well-defined self-assemblies with functional organic and/or inorganic counterions. In this work, we have

[†] Kyoto University.
[‡] Meijo University.
[§] Yamaguchi University.

(1) *Handbook of Nanostructured Materials and Nanotechnology*; Nalwa, H. S., Ed.; Academic Press: New York, 2000.
(2) *Nanomaterials Chemistry*; Rao, C. N. R., Mueller, A., Cheetham, A. K., Eds.; Wiley-VCH Verlag: Weinheim, 2007.
(3) Schaak, R. E.; Mallouk, T. E. *Chem. Mater.* **2002**, *14*, 1455–1471.
(4) Sasaki, T. *J. Ceram. Soc. Jpn.* **2007**, *115*, 9–16.
(5) Fang, M.; Kim, C. H.; Saupe, G. B.; Kim, H.-N.; Waraksa, C. C.; Miwa, T.; Fujishima, A.; Mallouk, T. E. *Chem. Mater.* **1999**, *11*, 1526–1532.
(6) Abe, R.; Shinohara, K.; Tanaka, A.; Hara, M.; Kondo, J. N.; Domen, K. *J. Mater. Res.* **1998**, *13*, 861–865.
(7) Sasaki, T.; Watanabe, M.; Hashizume, H.; Yamada, H.; Nakazawa, H. *J. Am. Chem. Soc.* **1996**, *118*, 8329–8335.
(8) Liu, Z.-h.; Ooi, K.; Kanoh, H.; Tang, W.-p.; Tomida, T. *Langmuir* **2000**, *16*, 4154–4164.

(9) Ebina, Y.; Sasaki, T.; Harada, M.; Watanabe, M. *Chem. Mater.* **2002**, *14*, 4390–4395.
(10) Domen, K.; Ebina, Y.; Ikeda, S.; Tanaka, A.; Kondo, J. N.; Maruya, K. *Catal. Today* **1996**, *28*, 167–174.
(11) Takagaki, A.; Sugisawa, M.; Lu, D.; Kondo, J. N.; Hara, M.; Domen, K.; Hayashi, S. *J. Am. Chem. Soc.* **2003**, *125*, 5479–5485.
(12) Wang, L.; Takada, K.; Kajiyama, A.; Onoda, M.; Michiue, Y.; Zhang, L.; Watanabe, M.; Sasaki, T. *Chem. Mater.* **2003**, *15*, 4508–4514.
(13) Sugimoto, W.; Iwata, H.; Yasunaga, Y.; Murakami, Y.; Takasu, Y. *Angew. Chem., Int. Ed.* **2003**, *42*, 4092–4096.
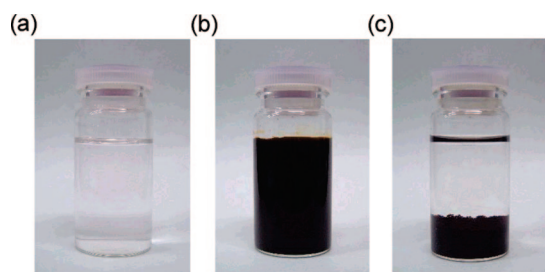
Figure 1. Photographs of (a) pale pink $MnCl_2$ aqueous solution, (b) dark brown colloidal suspension of MnO_2 monosheets obtained by adding a mixed aqueous solution of TMA·OH and H_2O_2 to the $MnCl_2$ solution, and (c) black potassium-type birnessite precipitated by adding a KCl aqueous solution to the colloidal suspension.

established a novel single-step route to synthesize the MnO_2 monosheets within a day in a high yield. During our study, a single-step synthesis of $Ti_{1-\delta}O_2$ monosheets with uniform shape and size was reported by Yoon and co-workers,[14] using titanium(IV) tetraisopropoxide in tetramethylammonium (TMA) hydroxide aqueous solution. While their processing requires the application of heat under reflux to access the $Ti_{1-\delta}O_2$ monosheets, our present reaction readily proceeds at room temperature (RT). In addition, MnO_2 monosheets have received much attention for their potential applications in electrochemistry and catalysis, mainly due to the low cost and safety hazards of manganese. Lamellar stacked Li/MnO_2 and layer-by-layer assembled poly-(ethyleneimide)/MnO_2, both of which are prepared from MnO_2 monosheets, have been employed as electrodes for lithium-ion batteries[12] and double-layer capacitors,[15] respectively, and exhibited improved performances associated with their porous structures. It is thus apparent that such rapid and facile RT processing promotes the work toward practical use of MnO_2 monosheets.

2. Results and Discussion

2.1. Formation of MnO_2 Monosheets. Our approach follows the preparation of lithium- and sodium-type birnessites by using hydrogen peroxide (H_2O_2) as an oxidizing agent for Mn^{2+} ions.[16−18] Here we used, in addition to H_2O_2, TMA·OH in an aqueous solution of manganese(II) chloride ($MnCl_2$, Figure 1a; see Supporting Information, Figure S1), which readily gave a dark brown suspension in open air at RT (Figure 1b). The observation of Tyndall light scattering in the suspension confirms the colloidal dispersion of the product, and no precipitation was observed in 3 days. Such a suspension was obtained even when trivalent manganese(III) acetylacetonate ($Mn(acac)_3$) was used instead of divalent $MnCl_2$, presumably as a reflection of the hydrolysis of $Mn(acac)_3$. Similarly, spinel $LiMn_2O_4$ and orthorhombic $LiMnO_2$ were formed by hydrolysis of $Mn(acac)_3$ in a LiOH aqueous solution.[19]

Because of the difficulties in confirming the presence of MnO_2 monosheets in the colloidal suspension, we observed the dried

aggregate using electron microscopy. Scanning electron microscopy (SEM) images of freeze-dried aggregates of the product showed a flexible flaky form with lateral dimension of micrometers, as shown in Figure 2a. The sheet-like structure was also evident from a tapping-mode atomic force microscopy (AFM) image of the sample deposited by spin-coating of the colloidal suspension onto a fluorinated mica substrate precoated with poly(ethyleneimine) (Figure 2c). The lateral dimension of the sample lies in the range of 50−500 nm, which is much larger than that of the $Ti_{1-\delta}O_2$ monosheets obtained by the single-step approach described by Yoon et al. (<30 nm).[14] The height profile scan demonstrates a fairly flat surface of the sheets with an approximate thickness of 0.9 nm. The dimensions are comparable to those of the MnO_2 monosheets obtained by the conventional processing,[20] suggesting a successful formation of the monosheets. Given the thickness of the MnO_2 monosheet (0.52 nm), hydration on both sides of the monosheets can reasonably explain the observed thickness, as discussed in ref 21. Furthermore, the AFM image displays stepwise structure with a step of ca. 0.7 nm, consistent with the thickness expected from the MnO_2 monosheet hydrated on the top. The most remarkable observation in this study is that the majority of the coverage area is composed of monosheets (Figure 2d). We note that replacing the TMA cation with a bulkier tetrabutylammonium cation while keeping the other conditions the same produces the similar results. When we used primary *n*-butylamine instead of quaternary tetraalkylammonium cations, on the other hand, the black precipitate of layered hybrid *n*-butylammonium/MnO_2 was readily obtained. This result will be reported in a separate paper.[22]

Figure 3 shows the absorption spectra in the range of 250−800 nm as a function of concentration of the colloidal suspension. An absorption band attributable to the d−d transition of Mn ions in the MnO_6 octahedra of the MnO_2 monosheets[19,23,24] was observed around 380 nm. This band follows Beer's law in the measured concentration range (inset of Figure 3), and the molar extinction coefficient at 380 nm is estimated to be $9.6 \times 10^3 \text{ M}^{-1} \text{ cm}^{-1}$, provided that the composition is $(TMA)_{0.20}MnO_2 \cdot 0.2H_2O$ (*vide infra*). The energy and intensity of the band are comparable to those obtained by the conventional multistep processing.[20]

A similar strategy to obtain metal oxide nanosheets without a high-temperature treatment was recently implemented by Oaki and Imai.[25] They employed ethylenediaminetetraacetate (EDTA) as chelating agent for Mn^{2+} ions so as to inhibit the rapid precipitation of $Mn(OH)_2$. The Mn^{2+} ions were oxidized slowly by dissolved oxygen in the solution. However, the precipitate is far from monosheets but consists of multilayers with a thickness of at least 10 nm (i.e., more than 10 layers), and the whole processing requires 3−5 days. In our processing, on the other hand, H_2O_2 serves as an oxidizing agent to form MnO_2 monosheets in alkaline medium, and TMA cations, previously

(14) Tae, E. L.; Lee, K. E.; Jeong, J. S.; Yoon, K. B. *J. Am. Chem. Soc.* **2008**, *130*, 6534−6543.

(15) Zhang, X.; Yang, W.; Evans, D. G. *J. Power Sources* **2008**, *184*, 695−700.

(16) Feng, Q.; Sun, E.; Yanagisawa, K.; Yamasaki, N. *J. Ceram. Soc. Jpn.* **1997**, *105*, 564−568.

(17) Feng, Q.; Higashimoto, Y.; Kajiyoshi, K.; Yanagisawa, K. *J. Mater. Sci. Lett.* **2001**, *20*, 269−271.

(18) Cai, J.; Liu, J.; Suib, S. L. *Chem. Mater.* **2002**, *14*, 2071−2077.

(19) Barriga, C.; Calero, A.; Morales, C. J.; Tirado, J. L. *React. Solids* **1989**, *7*, 263−271.

(20) Omomo, Y.; Sasaki, T.; Wang, L.; Watanabe, M. *J. Am. Chem. Soc.* **2003**, *125*, 3568−3575.

(21) Sasaki, T.; Ebina, Y.; Kitami, Y.; Watanabe, M.; Oikawa, T. *J. Phys. Chem. B* **2001**, *105*, 6116−6121.

(22) Kai, K.; Yoshida, Y.; Kageyama, H.; Saito, G.; et al., to be submitted.

(23) Gao, Q.; Giraldo, O.; Tong, W.; Suib, S. L. *Chem. Mater.* **2001**, *13*, 778−786.

(24) Wang, L.; Omomo, Y.; Sakai, N.; Fukuda, K.; Nakai, I.; Ebina, Y.; Takada, K.; Watanabe, M.; Sasaki, T. *Chem. Mater.* **2003**, *15*, 2873−2878.

(25) Oaki, Y.; Imai, H. *Angew. Chem., Int. Ed.* **2007**, *46*, 4951−4955.
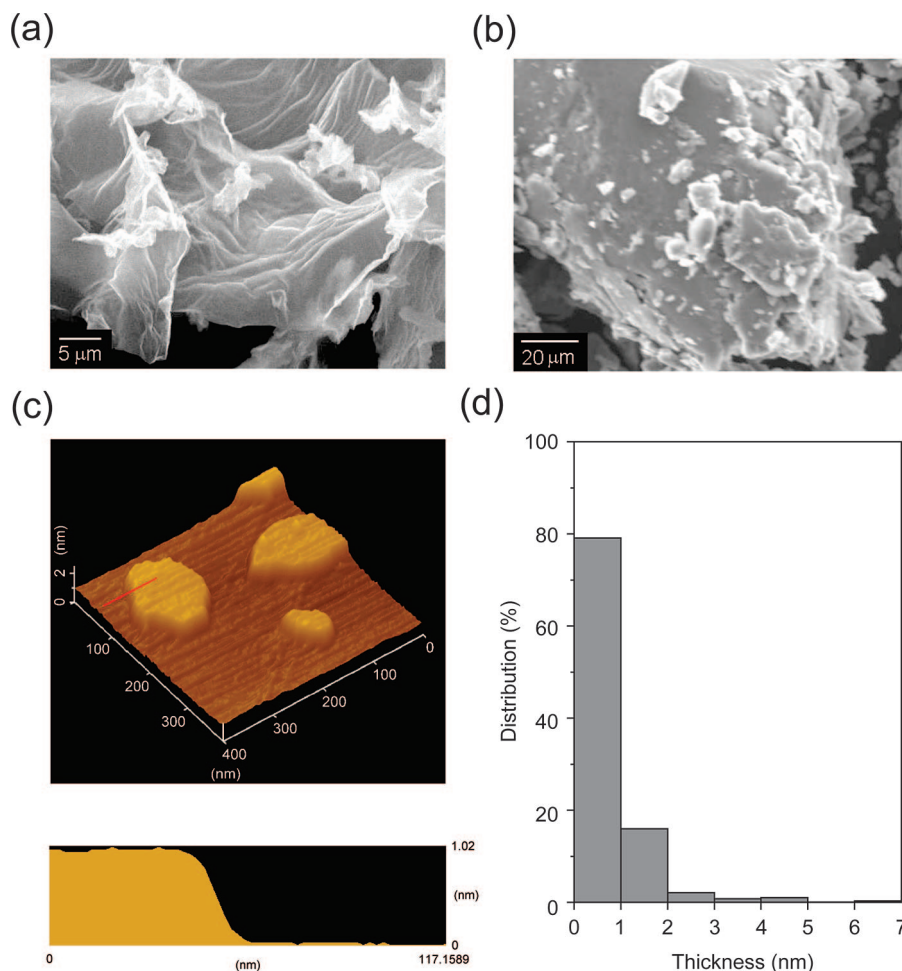
Figure 2. SEM images of (a) freeze-dried aggregate of MnO_2 monosheets and (b) self-assembled K/MnO_2. (c) Tapping-mode AFM image of MnO_2 monosheets and height profile along the red line in the image. The monosheets are deposited onto fluorinated mica substrate precoated with poly(ethyleneimine) by spin-coating (1000 rpm for 15 s and 2000 rpm for 30 s) of 0.1 g L^{-1} colloidal suspension. (d) Histogram of thickness of the MnO_2 sheets on the substrate.
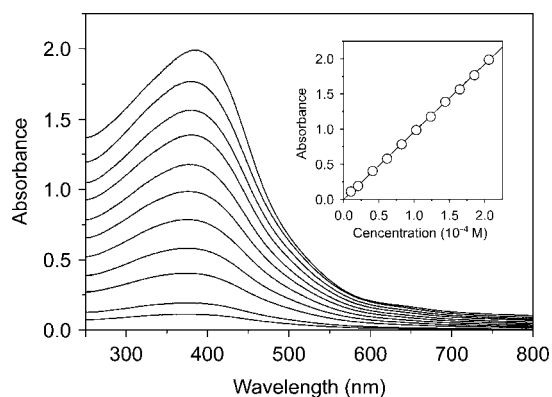

Figure 3. UV−vis absorption spectra of the colloidal suspension of MnO_2 monosheets as a function of the nanosheet concentration: from bottom to top, 1.03×10^{-5}, 2.06×10^{-5}, 4.12×10^{-5}, 6.18×10^{-5}, 8.24×10^{-5}, 1.03×10^{-4}, 1.24×10^{-4}, 1.44×10^{-4}, 1.65×10^{-4}, 1.85×10^{-4}, and 2.06×10^{-4} M. The inset shows the plot of absorbance at 380 nm against monosheet concentration, and the solid line corresponds to the fit indicating the molar extinction coefficient of 9.6×10^3 M^{-1} cm^{-1}.

used for the exfoliation of layered H/MnO_2,[8,26] would play an essential role during the course of two-dimensional growth of

the monosheets; namely, the cations serve not only to inhibit the flocculation of the monosheets but also to exfoliate the locally aggregated monosheets in the suspension. Although we do not have information about the mechanism of production of the MnO_2 monosheets, as the d−d absorption band appears and saturates within the measurement limit of our time acquisition measurement system (ca. 0.2 s), we believe that our rapid and facile processing promotes the practical use of the MnO_2 monosheets in lithium-ion batteries, catalysts, selective adsorbents, and so on, and also is generally applicable to the fabrication of other metal oxide monosheets.

2.2. Structural and Physical Properties of Dried Aggregate. In order to obtain further evidence of the formation of MnO_2 monosheets, powder X-ray diffraction (XRD) of a dried sample of the colloidal suspension, which was separated by filtration, washed with copious amounts of distilled water and methanol, and then air-dried at RT, was measured. The XRD pattern is indexed as a hexagonal unit cell and has intense (00*l*) reflections associated with the preferred orientation of the sample (Figure 4a), which is similar to that of the dried aggregate TMA/MnO_2 obtained by the conventional processing.[26,27] The interlayer spacing of 0.95 nm indicates the flocculation of the MnO_2 monosheets together with TMA and water molecules,[26,27] which

(26) Yang, X.; Makita, Y.; Liu, Z.-h.; Sakane, K.; Ooi, K. *Chem. Mater.* **2004**, *16*, 5581–5588.

(27) Brock, S. L.; Sanabria, M.; Suib, S. L.; Urban, V.; Thiyagarajan, P.; Potter, D. I. *J. Phys. Chem. B* **1999**, *103*, 7416–7428.
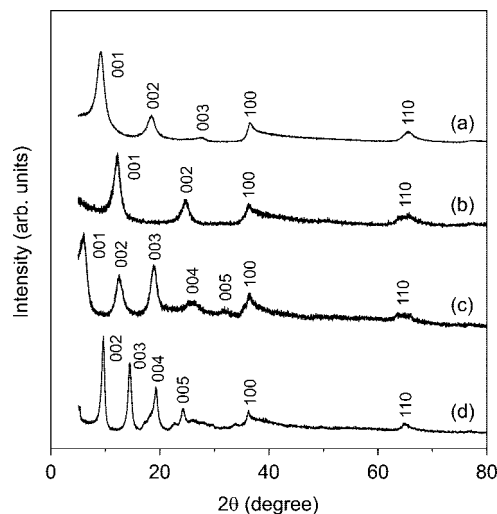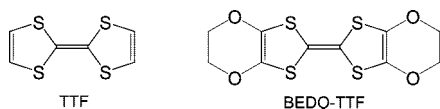
Figure 4. Powder X-ray diffraction patterns of (a) dried aggregate TMA/MnO_2, (b) self-assembled K/MnO_2, (c) self-assembled TTF/MnO_2, and (d) self-assembled BEDO-TTF/MnO_2.

Scheme 1. Molecular Structures of Tetrathiafulvalene (TTF) and Bis(ethylenedioxy)-Tetrathiafulvalene (BEDO-TTF)

should be driven mainly by electrostatic interactions between negatively charged monosheets and TMA cations. Together with this observation, the elemental analysis (Calcd: C, 9.12; H, 2.68; N, 2.66. Found: C, 9.16; H, 2.67; N, 2.69.) leads us to conclude that the composition of the dried aggregate is formulated as $(TMA)_{0.20}MnO_2 \cdot 0.2H_2O$, which yields the valence state on Mn of ca. $+3.8$.

Figure 5a displays the temperature dependence of DC susceptibility (χ) for the dried aggregate in an applied magnetic field of 1 kOe. Above 20 K, it follows the Curie–Weiss expression, $\chi = C(T - \theta)^{-1}$, with Curie constant ($C$) of 1.44 emu K mol^{-1} and Weiss temperature (θ) of -36.4 K. As seen in the inset of Figure 5a, a susceptibility cusp was observed around 10 K, below which there is a distinct difference between the zero-field-cooled (ZFC) and field-cooled (FC) susceptibilities. The cusp was also observed in both in-phase (χ') and out-of-phase (χ'') components of the AC susceptibility and shows an increase of ca. 1 K with increasing frequency (ν) on going from 1 Hz to 1 kHz (Figure 5b for χ'). The frequency shift in T_f (peak temperature of χ') is diagnostic for a glassy effect such as spin-glass or superparamagnetism and is defined as $\gamma = \Delta T_f/[T_f(0)\Delta(\log \nu)]$, where $T_f(0)$ is the peak temperature extrapolated at $\log \nu = 0$. The calculated small γ value (0.035) strongly indicates that the behavior is not due to the superparamagnetism, but arises from the spin-glass formation.[28] This behavior should be related to the geometrical frustration caused by the triangular arrangement of the mixed-valence $Mn^{4+/3+}$ ions in the MnO_2 layer. A similar trend was observed for K/MnO_2, H/MnO_2, and TMA/MnO_2 obtained by the conventional processing (Supporting Information, Figures S2–S4).

2.3. Self-Assembly of MnO_2 Monosheets. Since the MnO_2 monosheets have a negative charge, as mentioned above, the electrostatic interactions with organic and/or inorganic cations

would bring about self-assembly to yield lamellar aggregates using the present colloidal suspension. In the following, we present the preparation of lamellar aggregates formed with alkali and π-conjugated organic cations, and Langmuir–Blodgett (LB) films deposited onto hydrophilic silica substrate.

2.3.1. Potassium-Type Birnessite. A self-assembled potassium-type birnessite was readily precipitated in nearly quantitative yield by adding an excess of KCl to the colloidal suspension shown in Figure 1c. In comparison with the dried aggregate TMA/MnO_2, the XRD pattern (Figure 4b) and SEM image (Figure 2b) of the self-assembled K/MnO_2 indicate that it has a layered structure as well, but the interlayer spacing is greatly reduced to 0.70 nm, which is comparable to that of the potassium-type birnessite previously reported.[26] The K/Mn ratio was estimated to be 0.20 on the basis of energy-dispersive X-ray spectroscopy (EDS; Supporting Information, Figure S5), and the valence state on Mn of ca. $+3.8$ is in good agreement with that of the dried aggregate.

2.3.2. Organic–Inorganic Layered Hybrids. Layered hybrids composed of tetrathiafulvalene (TTF) and bis(ethylenedioxy)-TTF (BEDO-TTF) (Scheme 1), which have afforded a number of organic metals including superconductors,[29,30] were immediately obtained by adding powdered $(TTF)_3(BF_4)_2$[31] and $(BEDO-TTF)_2BF_4$ to the colloidal suspension. Taking the molecular lengths of TTF and BEDO-TTF as ca. 0.9 and 1.3 nm, respectively, the significantly expanded interlayer spacings of 1.45 and 1.84 nm (Figure 4c,d) suggest the formation of the layered hybrids with TTF analogues oriented almost perpendicular to the MnO_2 layers. According to the S/Mn ratios estimated from EDS (Supporting Information, Figures S6 and S7), the composition of the hybrids can be formulated as $(TTF)_{0.15}MnO_2 \cdot 1.0H_2O$ and $(BEDO-TTF)_{0.21}MnO_2 \cdot 1.6H_2O$, in which the water contents were estimated from thermogravimetric analyses. UV–vis absorption spectra of the hybrids dispersed in a compressed KBr disk show a low-energy band around 5×10^3 cm^{-1} (Supporting Information, Figures S8 and S9). This band can be assigned to the intermolecular transition between partially charged TTF analogues, suggesting that these hybrids can be potentially a metal,[29,30] though the semiconducting behavior observed was possibly due to the inhomogeneous packing of TTF analogues.

2.3.3. Langmuir–Blodgett (LB) Films. Figure 6a shows the surface pressure–area (π–A) isotherm of the diluted colloidal suspension of MnO_2 monosheets (0.01 g L^{-1}). A clear solid-condensed phase was observed, as was the case for $Ti_{1-\delta}O_2$ monosheets.[32] The LB films were fabricated on fused silica substrate by the LB deposition method without any amphiphilic additives at the air–water interface. UV–vis spectra of the films for each deposition process display an absorption band around 368 nm (Figure 6b), similar to those observed for the colloidal suspensions, and the absorbance of the band increases linearly with each deposition process (inset of Figure 6b). Since AFM observation of the film fabricated by a single deposition process reveals that the majority of the coverage area is composed of MnO_2 monosheets, it appears that about one layer of monosheets was transferred for each deposition process. The XRD pattern of the film with 30 layers, which displays a reflection at $2\theta =$

(28) Mydosh, J. A. *Spin Glass*; Taylor & Francis: London, 1993.

(29) Saito, G.; Yoshida, Y. *Bull. Chem. Soc. Jpn.* **2007**, *80*, 1–137.

(30) Horiuchi, S.; Yamochi, H.; Saito, G.; Sakaguchi, K.; Kusunoki, M. *J. Am. Chem. Soc.* **1996**, *118*, 8604–8622.

(31) Wudl, F. *J. Am. Chem. Soc.* **1975**, *97*, 1962–1963.

(32) Muramatsu, M.; Akatsuka, K.; Ebina, Y.; Wang, K.; Sasaki, T.; Ishida, T.; Miyake, K.; Haga, M. *Langmuir* **2005**, *21*, 6590–6595.
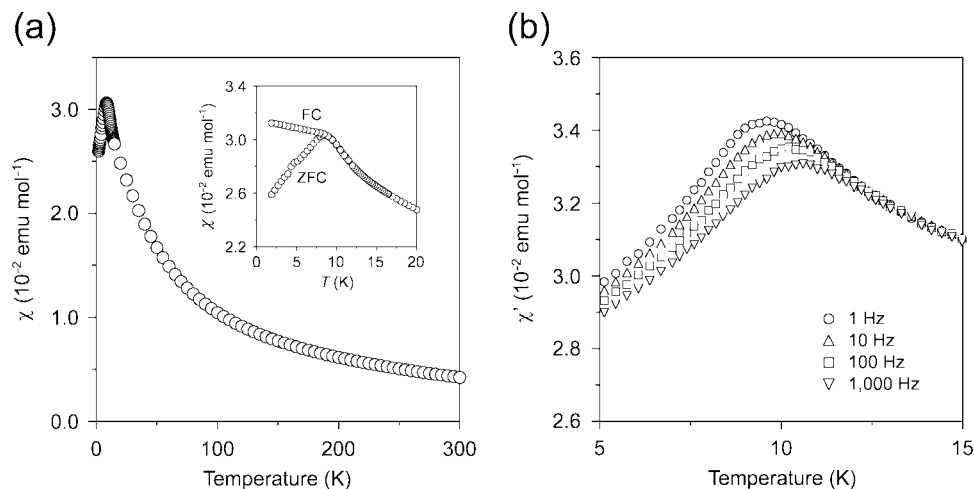
(a)

(b)

Figure 5. Temperature dependence of magnetic susceptibility of the dried aggregate TMA/MnO$_2$. (a) DC magnetic susceptibility (χ) under an applied magnetic field of 1 kOe. Above 20 K, the χ value follows the Curie−Weiss law with Curie constant of 1.44 emu K mol^{-1} and Weiss temperature of −36.4 K. The inset shows the low-temperature range of χ, showing the difference between the zero-field-cooled (ZFC) and field-cooled (FC) susceptibilities. (b) In-plane AC magnetic susceptibility (χ') at different frequencies (1, 10, 100, and 1000 Hz).
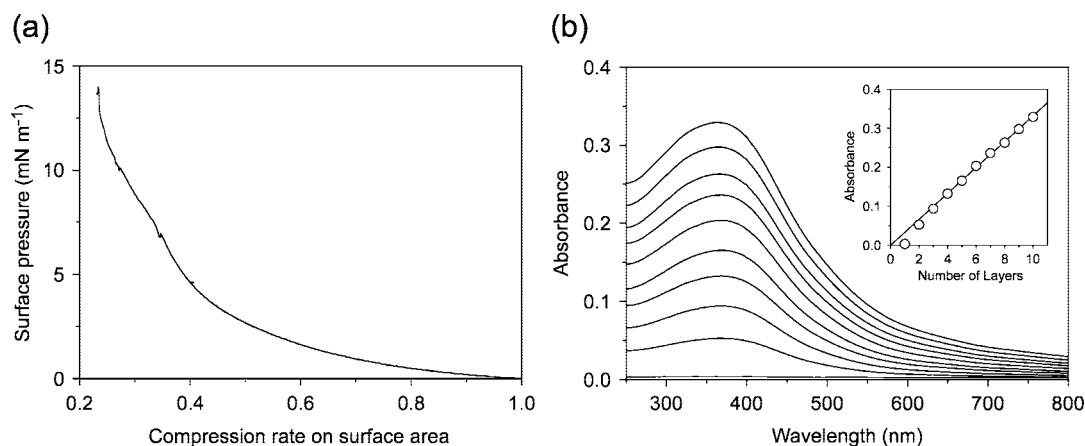
(a)

(b)

Figure 6. (a) Surface pressure−area ($\pi-A$) isotherm of MnO$_2$ monosheets in a diluted colloidal suspension (0.01 g L^{-1}). The initial surface area of the subphase was 130 cm^2. The values in the horizontal axis of the isotherm indicate the relative surface area against the initial one. (b) UV−vis absorption spectra of the LB films as a function of the number of layers (1−10). The inset shows the plot of absorbance at 368 nm against the number of layers.

12°, corresponding to an interlayer spacing of 0.73 nm (Supporting Information, Figure S10), confirms the regular stacking of the MnO$_2$ monosheets, although the nature of the interlayer cations is unclear at present.

3. Conclusions

In this study, we found a rapid and facile route to access a colloidal suspension of MnO$_2$ monosheets in a high yield. Although our single-step approach cuts the processing time to less than a day and eliminates the need for special equipment, the structural, spectroscopic, and magnetic properties of the products are comparable to those of MnO$_2$ monosheets (or their aggregate) obtained by the conventional multistep processing. Also, our process makes it possible to fabricate high-purity organic−inorganic layered hybrids and LB films composed of the MnO$_2$ monosheets. Further works, particularly on the applications of our processing into the fabrication of other metal oxide monosheets, are in progress.

4. Experimental Section

4.1. Measurements. SEM and EDS experiments were conducted with a JEOL JSM-5510LVN scanning electron microscope operated

at 20 kV. Samples are mounted on carbon tape. A Seiko SPA400 AFM instrument was employed to visualize the surface topography of the nanosheets. Measurements were carried out in tapping mode with a silicon-tip cantilever having a force constant of 20 N m^{-1}. Samples were deposited onto fluorinated mica substrate (Fluoro-Phologopite, Topy Industry Ltd.) precoated with poly(ethyleneimine) by spin-coating (1000 rpm for 15 s and 2000 rpm for 30 s) of a 0.1 g L^{-1} colloidal suspension. Powder XRD measurements were carried out with a MAC Science M18XHF diffractometer using Cu Kα radiation at a scanning rate of 0.01° s^{-1} in a 2θ range of 5−80°. UV−vis absorption spectra were taken in a quartz cell with light path length of 1 cm on a Shimadzu UV-3100 spectrophotometer (250−800 nm). Time acquisition of the absorption spectra was measured using an Ocean Optics HR-2000 spectrophotometer. FT-IR spectra were taken in dispersed KBr pellets on a Perkin-Elmer 1000 series spectrophotometer (400−7800 cm^{-1}). A Quantum Design MPMS-XL superconducting quantum interference device (SQUID) magnetometer was used to collect DC magnetic susceptibility data between 1.9 and 300 K. The AC magnetic susceptibilities for 1.9−20 K were determined in the range of 1 Hz to 1 kHz using a Quantum Design MPMS-5S SQUID magnetometer.

4.2. Synthesis. Solvents (water, methanol, acetonitrile, and chloroform) were distilled prior to use. MnCl$_2$·4H$_2$O (99.9%, Wako Pure Chemical), TMA·OH (1.0 M in H$_2$O, Aldrich), H$_2$O$_2$ (30 wt

% in H_2O, Santoku Chemical), and HBF_4 (48 wt % in H_2O, Aldrich) were commercially available and used without purification. Commercially available TTF was purified by sublimation twice. BEDO-TTF was synthesized according to the literature procedure[33] and recrystallized twice from cyclohexane. $(TTF)_3(BF_4)_2$ was prepared using the chemical oxidation of TTF by H_2O_2 in the presence of HBF_4 in acetonitrile, according to literature procedure.[31] (BEDO-TTF)$_2BF_4$ was prepared in the same manner as $(TTF)_3(BF_4)_2$.

4.2.1. Preparation of Colloidal Birnessite Monosheets. Typically, 20 mL of a mixed aqueous solution of 0.6 M TMA·OH and 3 wt % H_2O_2 was added to 10 mL of 0.3 M $MnCl_2$·4H$_2$O aqueous solution within 15 s. The resulting dark brown suspension was stirred vigorously overnight in the open air at RT, which is accompanied by O_2 gas generation. Dried aggregate was separated by filtration (Millipore, type-JH, 0.45 μm pore size), washed with copious amounts of distilled water and methanol, and then air-dried at RT. No trace of Cl was detected from EDS of the dried aggregate (Supporting Information, Figure S11).

4.2.2. Preparation of Self-Assembled Potassium-Type Birnessites. Self-assembly of MnO_2 monosheets was induced by mixing the colloidal suspension of the monosheets with a KCl aqueous solution. Typically, 50 mL of 1 M KCl aqueous solution was added dropwise within 1 h to 50 mL of the colloidal suspension of MnO_2 monosheets (2×10^{-2} M) at 40 °C. Immediately after the addition, flocculation occurred in the mixed solution. After the solution was left to stand at RT for a week, the resulting black precipitate was filtered off, washed with copious amounts of distilled water and methanol, and air-dried at RT (yield 94%). The K/Mn ratio was estimated to be 0.20 on the basis of EDS (Figure S5).

4.2.3. Preparation of Self-Assembled Organic−Inorganic Layered Hybrid TTF/MnO$_2$. Typically, 0.50 g (0.64 mmol) of powdered $(TTF)_3(BF_4)_2$ was added to 300 mL of the colloidal suspension of MnO_2 monosheets (3×10^{-3} M) during N_2 bubbling at RT. After a few minutes of stirring, flocculation occurred in the mixed solution. The resulting black precipitate was filtered off, washed with acetonitrile, and air-dried at RT (yield 78%). The TTF/Mn ratio was estimated to be 0.15 on the basis of EDS (Figure S6), and the IR absorption spectrum indicates no trace of BF_4 anions (Supporting Information, Figure S12). Layered hybrid BEDO-TTF/MnO_2 was prepared by a procedure similar to that for TTF/MnO_2 as described in the Supporting Information.

4.2.4. Fabrication of LB Films. Fused silica substrates for depositing the films were cleaned with detergent followed by several rinses with water, and sonicated in fresh water three times for 30 min each. Their surfaces were made hydrophilic by treating with piranha solution (H_2O_2:H_2SO_4 = 7:3) for 90 min, followed by sonication and rinsing in water. The $\pi-A$ isotherm measurements and film fabrications employed a USI Co. Ltd. model FDS-23 LB trough equipped with a Wilhelmy plate for pressure sensing. A diluted aqueous suspension of MnO_2 monosheets (0.01 g L^{-1}) was used as a subphase. After the suspension was left to stand for 1 h, the surface of the subphase was compressed at a rate of 5 cm^2 min^{-1} by moving the barrier. The compressed film was deposited onto hydrophilic silica substrate at a surface pressure of 10 mN m^{-1} by the vertical deposition method. All experiments were carried out at 20 °C, and high-purity water (<0.1 μS s^{-1}) was used for all operations.

Supporting Information Available: Detailed characterization of the products. This material is available free of charge via the Internet at http://pubs.acs.org.

JA804503F

(33) Suzuki, T.; Yamochi, H.; Srdanov, G.; Hinkelmann, K.; Wudl, F. *J. Am. Chem. Soc.* **1989**, *111*, 3108–3109.